

# Detecting Heavy Higgs Bosons from Natural SUSY at a 100 TeV Hadron Collider

Howard Baer<sup>\*</sup> and Chung Kao<sup>†</sup>

*Homer L. Dodge Department of Physics and Astronomy,  
University of Oklahoma, Norman, OK 73019, USA*

Vernon Barger<sup>‡</sup>

*Department of Physics, University of Wisconsin, Madison, WI 53706, USA*

Rishabh Jain<sup>§</sup> and Dibyashree Sengupta<sup>¶</sup>

*Department of Physics, National Taiwan University, Taipei, Taiwan 10617, R.O.C*

Xerxes Tata<sup>\*\*</sup>

*Department of Physics, University of Hawaii, Honolulu, HI 96822, USA*

(Dated: April 18, 2022)

## Abstract

Supersymmetric models with radiatively-driven naturalness (RNS) enjoy low electroweak fine-tuning whilst respecting LHC search limits on gluinos and top squarks and allowing for  $m_h \simeq 125$  GeV. While the heavier Higgs bosons  $H$ ,  $A$  may have TeV-scale masses, the SUSY conserving  $\mu$  parameter must lie in the few hundred GeV range. Thus, in natural SUSY models there should occur large heavy Higgs boson branching fractions to electroweakinos, with Higgs boson decays to higgsino plus gaugino dominating when they are kinematically accessible. These SUSY decays can open up new avenues for discovery. We investigate the prospects of discovering heavy neutral Higgs bosons  $H$  and  $A$  decaying into light plus heavy chargino pairs which can yield a four isolated lepton plus missing transverse energy signature at the LHC and at a future 100 TeV  $pp$  collider. We find that discovery of heavy Higgs decay to electroweakinos via its  $4\ell$  decay mode is very difficult at HL-LHC. For FCC-hh or SPPC, we study the  $H$ ,  $A \rightarrow$  SUSY reaction along with dominant physics backgrounds from the Standard Model and devise suitable selection requirements to extract a clean signal for FCC-hh or SPPC with  $\sqrt{s} = 100$  TeV, assuming an integrated luminosity of  $15 \text{ ab}^{-1}$ . We find that while a conventional cut-and-count analysis yields a signal statistical significance greater than  $5\sigma$  for  $m_{A,H} \sim 1.1 - 1.65$  TeV, a boosted-decision-tree analysis allows for heavy Higgs signal discovery at FCC-hh or SPPC for  $m_{A,H} \sim 1 - 2$  TeV.

PACS numbers:

<sup>\*</sup>Electronic address: [baer@nhn.ou.edu](mailto:baer@nhn.ou.edu)

<sup>†</sup>Electronic address: [Chung.Kao@ou.edu](mailto:Chung.Kao@ou.edu)

<sup>‡</sup>Electronic address: [barger@pheno.wisc.edu](mailto:barger@pheno.wisc.edu)

<sup>§</sup>Electronic address: [rishabh.jain@hep1.phys.ntu.edu.tw](mailto:rishabh.jain@hep1.phys.ntu.edu.tw)

<sup>¶</sup>Electronic address: [dsengupta@phys.ntu.edu.tw](mailto:dsengupta@phys.ntu.edu.tw)

<sup>\*\*</sup>Electronic address: [tata@phys.hawaii.edu](mailto:tata@phys.hawaii.edu)

## I. INTRODUCTION

With the discovery of the 125 GeV Standard Model-like Higgs boson at LHC [1], all the particle states required by the Standard Model (SM) have been confirmed. And yet, many mysteries of nature still remain unsolved. Supersymmetric extensions of the SM are highly motivated in that they offer a solution to the gauge hierarchy problem (GHP) [2] which arises from the quadratic sensitivity of the Higgs boson mass to high scale physics. SUSY models are also supported indirectly by various precision measurements within the SM: 1. the weak scale gauge couplings nearly unify under renormalization group evolution at energy scale  $m_{GUT} \simeq 2 \times 10^{16}$  GeV in the MSSM, but not the SM [3], 2. the measured value of top quark falls within the range needed to initiate a radiative breakdown of electroweak symmetry in the MSSM [4], 3. the measured value of Higgs boson mass  $m_h \simeq 125$  GeV falls within the narrow range of MSSM predicted values [5], and 4. precision electroweak measurements actually favor *heavy SUSY* over the SM [6].

Recent LHC searches with  $\sqrt{s} = 13$  TeV and integrated luminosity  $L = 139 \text{ fb}^{-1}$  have put lower bounds on the mass of the gluino of about 2.2 TeV [7, 8] and on the mass of top squark of about 1.1 TeV [9, 10]. These limits, which have been obtained using simplified model analyses assuming that the sparticle spectrum is not compressed, fall well above upper bounds derived from early naturalness considerations [11–15]. However, the naturalness estimates from the log-derivative measure are highly dependent on what one regards as independent parameters of the theory [16].<sup>1</sup> We adopt the more conservative quantity  $\Delta_{EW}$ , that allows for the possibility of correlations among model parameters, as a measure of naturalness [17].  $\Delta_{EW}$  can be extracted from Eq. (1),

$$\frac{m_Z^2}{2} = \frac{m_{H_d}^2 + \Sigma_d^d - (m_{H_u}^2 + \Sigma_u^u) \tan^2 \beta}{\tan^2 \beta - 1} - \mu^2, \quad (1)$$

which relates the mass of Standard Model  $Z$  boson to SUSY Lagrangian parameters at the weak scale and is obtained from the minimization conditions of the MSSM scalar potential [18]. The electroweak fine-tuning parameter  $\Delta_{EW}$  is defined by,

$$\Delta_{EW} \equiv (\max|\text{term on RHS of Eq. 1}|)/(m_Z^2/2). \quad (2)$$

The condition for naturalness is that the maximal contribution to the  $Z$  mass should be within a factor of several of its measured value. We consider spectra that yield  $\Delta_{EW} > \Delta_{EW}(\max) = 30$  as fine-tuned [19].

This condition then requires :

- the SUSY-conserving  $\mu$  parameter  $\approx 110\text{-}350$  GeV;
- the up-Higgs soft mass term  $m_{H_u}^2$  may be large at high scales but can be radiatively-driven to (negative) natural values  $\sim -m_{weak}^2$  at the weak scale;

---

<sup>1</sup> The various soft SUSY breaking terms which are adopted for the log-derivative measure are introduced to parameterize one's ignorance of how soft terms arise. In more UV-complete models such as string theory, then the various soft terms are all calculable and not independent. Ignoring this could result in an over-estimate of the UV sensitivity of the theory by orders of magnitude.

- The finite radiative correction  $\Sigma_u^u(\tilde{t}_{1,2})$  has an upper bound of  $(350 \text{ GeV})^2$  which is possible even for  $m_{\tilde{t}}$  up to 3 TeV and  $m_{\tilde{g}} \approx 6 \text{ TeV}$  [20], compatible with LHC constraints;
- the heavy Higgs masses  $m_{A,H,H^\pm} \sim |m_{H_d}|$ , with  $|m_{H_d}|/\tan\beta \sim \frac{m_Z}{\sqrt{2}}\sqrt{\Delta_{EW}}$ .

We thus see that naturalness requires [21]

$$m_A \lesssim \frac{m_Z \tan\beta \sqrt{\Delta_{EW}(\text{max})}}{\sqrt{2}}, \quad (3)$$

and further, that for  $\tan\beta \sim 5 - 50$ , the heavy Higgs boson masses may be expected to lie in the (multi)-TeV range for an electroweak fine-tuning of up to a part in thirty.

The conditions mentioned above are satisfied in radiatively-driven natural supersymmetric (RNS) models. One of the features of RNS models is that the heavier Higgs bosons may lie in the multi-TeV range while at least some of the electroweakinos (EWinos) are below a few hundred GeV. This means that generically we expect that in natural SUSY models the supersymmetric decay modes of the heavy Higgs bosons should be kinematically accessible, and often with branching fractions comparable to SM decay modes. If SUSY decay modes of the heavy Higgs bosons are allowed, then 1. SM search modes will be suppressed due to the presence of the SUSY decay modes and 2. potentially new avenues for heavy Higgs discovery may open up. This situation was investigated long ago under the supposition that the lightest EWinos were predominantly gaugino-like [22]. In Ref. [23], a lucrative  $A, H \rightarrow \tilde{\chi}_2^0 \tilde{\chi}_2^0 \rightarrow 4\ell + \cancel{E}_T$  search mode was identified for LHC. However, in RNS models, we expect instead that the lightest EWinos to be dominantly higgsino-like.

Thus, we explore here a new possible heavy Higgs discovery channel for SUSY models with light higgsinos. We identify the dominant new SUSY decay mode for heavy neutral Higgs in natural SUSY models as  $H, A \rightarrow \tilde{\chi}_1^\pm \tilde{\chi}_2^\mp$  that proceeds with full gauge strength<sup>2</sup> (provided that the decay is kinematically allowed). Allowing for chargino cascade decays, then an analogous clean  $4\ell + \cancel{E}_T$  signature can be found. It includes leptons from the lighter chargino decay  $\tilde{\chi}_1^\pm \rightarrow \ell^\pm \bar{\nu}_\ell \tilde{\chi}_1^0$  where the final state leptons are expected to be quite soft in the chargino rest frame due to the expected small mass gap  $m_{\tilde{\chi}_1^\pm} - m_{\tilde{\chi}_1^0}$ . However, due to  $m_{H,A}$  lying in the TeV-range, these final state leptons may be strongly boosted and thus can potentially contribute to the signal. In this paper, we examine the particular reaction  $pp \rightarrow H, A \rightarrow \tilde{\chi}_1^\pm \tilde{\chi}_2^\mp \rightarrow 4\ell + \cancel{E}_T$  where due to the heavy Higgs resonance, we expect  $m_T(4\ell, \cancel{E}_T)$  to be kinematically bounded by  $m_{H,A}$  (see Fig. 1). While this reaction will prove difficult to extract at HL-LHC – due in part to the several leptonic branching fractions which are required – we find that discovery in this channel should be possible at the FCC-hh[24] or SPPC[25]  $pp$  collider with  $\sqrt{s} \sim 100 \text{ TeV}$  and  $15 \text{ ab}^{-1}$  of integrated luminosity. The FCC-hh or SPPC collider has emerged as the next target hadron collider for CERN after HL-LHC in the updated European strategy report [26].

To be specific, we will adopt a RNS benchmark (BM) point as listed in Table I, as generated using Isajet 7.88 [27]. This BM comes from the two-extra-parameter non-universal Higgs model NUHM2 [28]. The NUHM2 model parameter space is given by

<sup>2</sup> By full gauge strength, we only mean that the Higgs scalar-higgsino-gaugino vertex is unsuppressed. We recognize, of course, that the overall coupling of the heavy Higgs sector to the gauge boson sector is suppressed by mixing angles in the scalar Higgs sector.

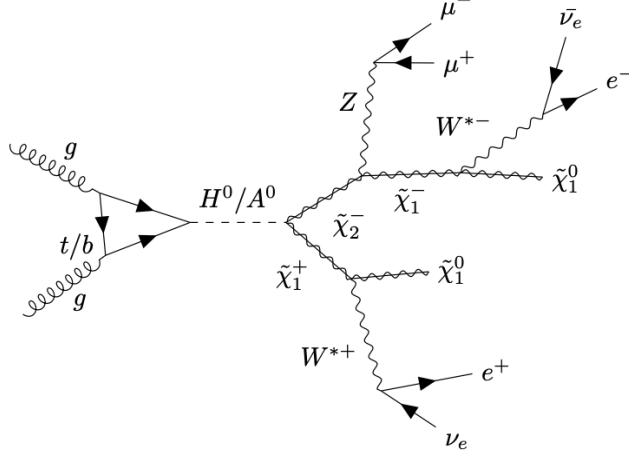


FIG. 1: Feynman diagram for  $gg \rightarrow H, A(\rightarrow \tilde{\chi}_2^\pm \tilde{\chi}_1^\mp \rightarrow 4\ell + \cancel{E}_T) + X$  production; there is a similar diagram for  $H, A$  production via  $b\bar{b}$  fusion.

$m_0, m_{1/2}, A_0, \tan \beta$  along with non-universal Higgs mass soft terms  $m_{H_u} \neq m_{H_d} \neq m_0$ . Using the EW minimization conditions, it is convenient to trade the high scale soft terms  $m_{H_u}, m_{H_d}$  for the weak scale parameters  $\mu$  and  $m_A$ . This BM point yields  $m_{\tilde{g}} \simeq 2.4$  TeV, somewhat beyond the LHC lower limit of 2.2 TeV obtained from a *simplified model analysis*. The heavy neutral Higgs scalars have mass  $m_{H,A} \sim 1.2$  TeV which is somewhat beyond the recent ATLAS limit[29] that requires  $m_{H,A} \gtrsim 1$  TeV for  $\tan \beta = 10$  via an  $H, A \rightarrow \tau^+ \tau^-$  search at  $\sqrt{s} = 13$  TeV and  $139 \text{ fb}^{-1}$  of integrated luminosity (while assuming no SUSY decay modes of the heavy Higgs bosons). Also, the SUSY  $\mu$  parameter is taken to be  $\mu = 200$  GeV so that the BM point lies just beyond the recent analyses of the *soft dilepton* plus monojet higgsino signal[30]. For the listed BM point, the lighter EWinos  $\tilde{\chi}_{1,2}^0$  and  $\tilde{\chi}_1^\pm$  are higgsino-like while  $\tilde{\chi}_3^0$  is bino-like and  $\tilde{\chi}_4^0$  and  $\tilde{\chi}_2^\pm$  are wino-like.

### A. Review of some previous related work and plan for this work

SUSY Higgs boson decays to EWinos were first calculated in Baer *et al.* Ref. [31]. A more comprehensive treatment was given in Gunion *et al.* [32] and Gunion and Haber [33]. Griest and Haber [34] considered the effect of invisible Higgs decays  $H \rightarrow \tilde{\chi}_1^0 \tilde{\chi}_1^0$ . In Kunszt and Zwirner Ref. [35], the phenomenology of SUSY Higgs bosons in the  $m_A$  vs.  $\tan \beta$  plane with just SM decay modes was considered in light of the important radiative corrections to  $m_h$ . The  $m_A$  vs.  $\tan \beta$  plane was mapped including the effects of Higgs to SUSY decays in Baer *et al.* Ref. [22] where diminution of SM Higgs decay channels due to SUSY modes was considered along with the potential for new discovery channels arising from the SUSY decay modes. In Ref. [23], the discovery channel  $H, A \rightarrow \tilde{\chi}_2^0 \tilde{\chi}_2^0 \rightarrow 4\ell + \cancel{E}_T$  was examined. In Djouadi *et al.* [36], SUSY decays of heavy Higgs bosons at  $e^+e^-$  colliders were considered. Barger *et al.* in Ref. [37] examined  $s$ -channel production of SM and SUSY Higgs bosons at muon colliders. In Belanger *et al.* [38], SUSY decays of Higgs bosons at LHC were examined. Choi *et al.*[39] examined the effects of CP violating phases on Higgs to SUSY decays. In Ref. [40], a CMS study of  $H, A \rightarrow \tilde{\chi}_2^0 \tilde{\chi}_2^0 \rightarrow 4\ell + \cancel{E}_T$  was performed. In Ref. [41], signals from

parameter	NUHM2
$m_0$	5 TeV
$m_{1/2}$	1.0 TeV
$A_0$	-8.3 TeV
$\tan \beta$	10
$\mu$	200 GeV
$m_A$	1.2 TeV
$m_{\tilde{g}}$	2423 GeV
$m_{\tilde{u}_L}$	5293 GeV
$m_{\tilde{u}_R}$	5439 GeV
$m_{\tilde{e}_R}$	4804 GeV
$m_{\tilde{t}_1}$	1388 GeV
$m_{\tilde{t}_2}$	3722 GeV
$m_{\tilde{b}_1}$	3756 GeV
$m_{\tilde{b}_2}$	5150 GeV
$m_{\tilde{\tau}_1}$	4727 GeV
$m_{\tilde{\tau}_2}$	5097 GeV
$m_{\tilde{\nu}_\tau}$	5094 GeV
$m_{\tilde{\chi}_1^\pm}$	208.4 GeV
$m_{\tilde{\chi}_2^\pm}$	856.7 GeV
$m_{\tilde{\chi}_1^0}$	195.4 GeV
$m_{\tilde{\chi}_2^0}$	208.5 GeV
$m_{\tilde{\chi}_3^0}$	451.7 GeV
$m_{\tilde{\chi}_4^0}$	867.9 GeV
$m_h$	125.0 GeV
$\Omega_{\tilde{z}_1}^{std} h^2$	0.011
$BF(b \rightarrow s\gamma) \times 10^4$	3.2
$BF(B_s \rightarrow \mu^+\mu^-) \times 10^9$	3.8
$\sigma^{SI}(\tilde{\chi}_1^0, p)$ (pb)	$3.1 \times 10^{-9}$
$\sigma^{SD}(\tilde{\chi}_1^0, p)$ (pb)	$6.1 \times 10^{-5}$
$\langle \sigma v \rangle _{v \rightarrow 0}$ (cm <sup>3</sup> /sec)	$2.0 \times 10^{-25}$
$\Delta_{EW}$	25.5

TABLE I: Input parameters (TeV) and masses (GeV) for a SUSY benchmark point from the NUHM2 model with  $m_t = 173.2$  GeV using Isajet 7.88 [27].

$H, A \rightarrow 4\ell + \cancel{E}_T$  were examined including *all* SUSY cascade decays of heavy Higgs bosons in scenarios where the  $\tilde{\chi}_1^0$  was bino-like. In Bae *et al.* [21], the impact of natural SUSY with light higgsinos on SUSY Higgs phenomenology was examined and natural regions of the  $m_A$  vs.  $\tan \beta$  plane were displayed along with relevant SUSY Higgs branching fractions. The LHC SUSY Higgs signatures  $H, A \rightarrow mono - X + \cancel{E}_T$  (where  $X = W, Z, h$ ) were examined against huge SM backgrounds. In Bae *et al.* Ref. [42], the effect of natural SUSY on Higgs coupling measurements  $\kappa_i$  was examined. In Barman *et al.* [43], SUSY Higgs branching fractions and  $mono - X + \cancel{E}_T$  signatures were examined at LHC for several benchmark points along with a Higgs to SUSY trilepton signature. In Ref. [44], six MSSM SUSY Higgs

benchmark points were proposed for LHC search studies, including one with a low, natural value of  $\mu$  (which seems now to be LHC-excluded). Gori, Liu and Shakya examined SUSY Higgs decays to EWinos and to stau pairs in Ref. [45]. In Adhikary *et al.* [46], Higgs decay to EWinos at LHC were examined, especially the  $Z + \cancel{E}_T$  and  $h + \cancel{E}_T$  signatures along with the possibility of Higgs decays to long-lived charged particles (LLCPs).

## B. Plan for this paper

In the present paper, we examine Higgs decays to SUSY particles in natural SUSY models with light higgsinos. In particular, in light of the large SM backgrounds for  $mono - X + \cancel{E}_T$  searches, we examine the viability of resurrecting the  $H, A \rightarrow 4\ell + \cancel{E}_T$  signature. In the natural SUSY case, this signature could arise from  $H, A \rightarrow \tilde{\chi}_1^\pm \tilde{\chi}_2^\mp$  followed by  $\tilde{\chi}_2^\pm \rightarrow Z \tilde{\chi}_1^\pm$ . The  $Z \rightarrow \ell^+ \ell^-$  decay should be easily visible but the leptons from  $\tilde{\chi}_1^\pm \rightarrow \ell \nu \tilde{\chi}_1^0$  are typically very soft in the  $\tilde{\chi}_1^\pm$  rest frame. Owing to the TeV scale values of  $m_{H,A}$ , these otherwise soft leptons may be boosted to detectable levels. While such a complicated decay channel appears intractable at HL-LHC, the FCC-hh or SPPC operating at  $\sqrt{s} \sim 100$  TeV and  $15 \text{ ab}^{-1}$  should allow for discovery for  $m_{H,A} \sim 1 - 2$  TeV with advanced machine learning (ML) techniques; here we have used boosted decision trees as an illustration.<sup>3</sup>

The remainder of this paper is organized as follows. In Sec. II, we present  $s$ -channel production rates for heavy Higgs bosons at LHC14 and at FCC-hh or SPPC. In Sec. III, we discuss the heavy Higgs branching fractions that are expected in natural SUSY models and we motivate our particular four lepton SUSY Higgs discovery channel. In Sec. IV, we discuss leading SM backgrounds to the  $H, A \rightarrow 4\ell + \cancel{E}_T$  signal channel. In Sec. V, we perform a cut-based analysis while in Sec. VI we show one can do much better by invoking a boosted-decision-tree (BDT) analysis. In Sec. VII, we summarize our main conclusions.

## II. HEAVY HIGGS PRODUCTION AT LHC AND FCC-HH OR SPPC

Here, we will focus on the  $s$ -channel heavy neutral Higgs boson production reactions  $pp \rightarrow H, A$  which occurs via the gluon-gluon and  $b\bar{b}$  fusion subprocesses. Other reactions such as  $pp \rightarrow qqH$  (VV fusion reactions)  $WH, ZH$  and  $t\bar{t}H$  all occur at lower rates [48] and also lead to different final state topologies. Hence, we will not include these in our analysis.

In Fig. 2, we show the heavy neutral Higgs production cross sections at next-to-next-to-leading order (NNLO) in QCD. We adopt the SusHi program to generate these results [47]. Higher order QCD corrections typically boost these cross sections above their leading order estimates. Frame (a) shows results for  $\sqrt{s} = 14$  TeV while frame (b) shows results for  $\sqrt{s} = 100$  TeV. We see that even for  $\tan \beta = 10$ , heavy Higgs boson production via  $b\bar{b}$  fusion dominates that from gluon fusion. From frame (a), we see that for  $m_A \sim 800$  GeV, the total production cross sections occur for both  $H$  and  $A$  production at the  $\sim 40$  fb level. As  $m_A$  increases, the rates fall and are already below the 0.2 fb level for  $m_A \gtrsim 2$  TeV. We

<sup>3</sup> Since one of our goals is to illustrate how ML techniques may help to eke out a signal that lies below the discovery limit using standard cut-and-count analyses if the Higgs boson is very massive, we have confined our study to the signal in this single channel, and for simplicity carried out our calculations using parton level simulations.



can anticipate that once we fold in various leptonic branching fractions and include detector acceptances, we will not expect very high rates for multi-lepton signals from heavy neutral SUSY Higgs bosons at LHC14. In frame (b), we show the results for  $\sqrt{s} = 100$  TeV. Here, the cross sections are increased by factors of 70-500 as  $m_A$  varies from 800-2000 GeV.

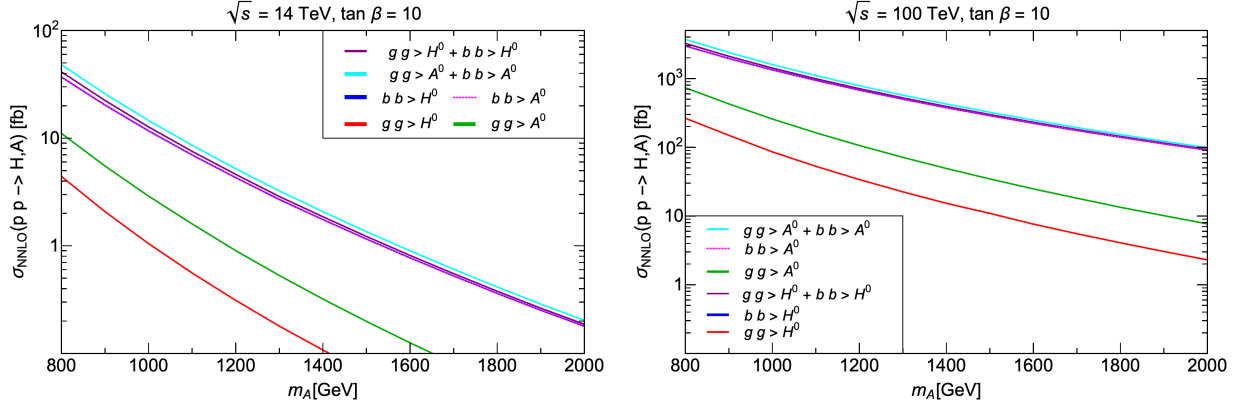


FIG. 2:  $\sigma_{NNLO}(pp \rightarrow H, A + X)$  for  $s$ -channel heavy neutral Higgs boson production reactions via  $gg$  and  $b\bar{b}$  fusion versus  $m_A$  for (a)  $\sqrt{s} = 14$  and (b)  $\sqrt{s} = 100$  TeV. We take  $\tan \beta = 10$ . Results are from SusHi[47].

### III. HEAVY HIGGS AND SPARTICLE BRANCHING FRACTIONS

In this Section, we present some updated heavy neutral and charged Higgs branching fractions which we extract from the Isajet 7.88 code [27]. We adopt the benchmark point from Table I except now we allow the heavy Higgs mass  $m_A$  to vary. In frame (a), we show branching fractions for the heavy neutral scalar  $H$ . At low  $m_H$ , the SM modes  $H \rightarrow b\bar{b}$ ,  $\tau\bar{\tau}$  and  $t\bar{t}$  are dominant, with their exact values depending on  $\tan \beta$  (large  $\tan \beta$  enhances the  $b\bar{b}$  and  $\tau\bar{\tau}$  modes). For  $m_H \sim 400 - 650$  GeV, the SM modes are still dominant even though the light electroweakino modes are open. We can understand this by examining the Higgs sector Lagrangian in the notation of Ref. [18], Sec. 8.4:

$$\mathcal{L} \ni -\sqrt{2} \sum_{i,A} \mathcal{S}_i^\dagger g t_A \bar{\lambda}_A \frac{1 - \gamma_5}{2} \psi_i + h.c. \quad (4)$$

where  $\mathcal{S}_i$  labels various matter and Higgs scalars (labeled by  $i$ ),  $\psi_i$  is the fermionic superpartner of  $\mathcal{S}_i$ , and  $\lambda_A$  is the gaugino with gauge index  $A$ . Also,  $g$  is the gauge coupling for the gauge group and  $t_A$  are the corresponding gauge group generator matrices. Letting  $\mathcal{S}_i$  be the Higgs scalar fields, then we see that the Higgs-EWino coupling is maximal when there is little mixing in that the Higgs fields couple directly to gaugino plus higgsino. Back in Fig. 3(a), for  $m_H$  small, then the only open decay modes are  $H$  to higgsino plus higgsino, and so the coupling must be dynamically suppressed because the gaugino component of the lightest EWinos is very small. Thus the SM modes are still dominant. As  $m_H$  increases, then the decay to gaugino plus higgsino turns on and the above coupling is unsuppressed (as has also been noted in footnote 2, above). For our choice of SUSY parameters, this happens around  $m_H \sim 650$  GeV for  $H$  decay to higgsino plus bino and around  $m_H \sim 1050$  GeV for  $H$  decay

to wino plus higgsino. Since the latter coupling involves the larger  $SU(2)_L$  gauge coupling, the decay  $H \rightarrow$  wino plus higgsino ultimately dominates the branching fraction once it is kinematically allowed. Thus, for  $m_H \gtrsim 1250$  GeV,  $H \rightarrow \tilde{\chi}_1^\pm \tilde{\chi}_2^\mp$  dominates the branching fraction (blue curve), while decays of  $H$  to the lighter neutral higgsino-like neutralino plus the heavier neutral wino or bino-like neutralino (green curve) have a branching fraction about half as large. In this range of  $m_H$ , the SM  $H$  decay modes are severely depressed from their two-Higgs doublet (non-SUSY) expectation. This will make heavy Higgs detection via  $t\bar{t}$ ,  $b\bar{b}$  and  $\tau\bar{\tau}$  much more difficult. On the other hand, it opens up new discovery channels by searching for the dominant  $H \rightarrow$  EWino modes.

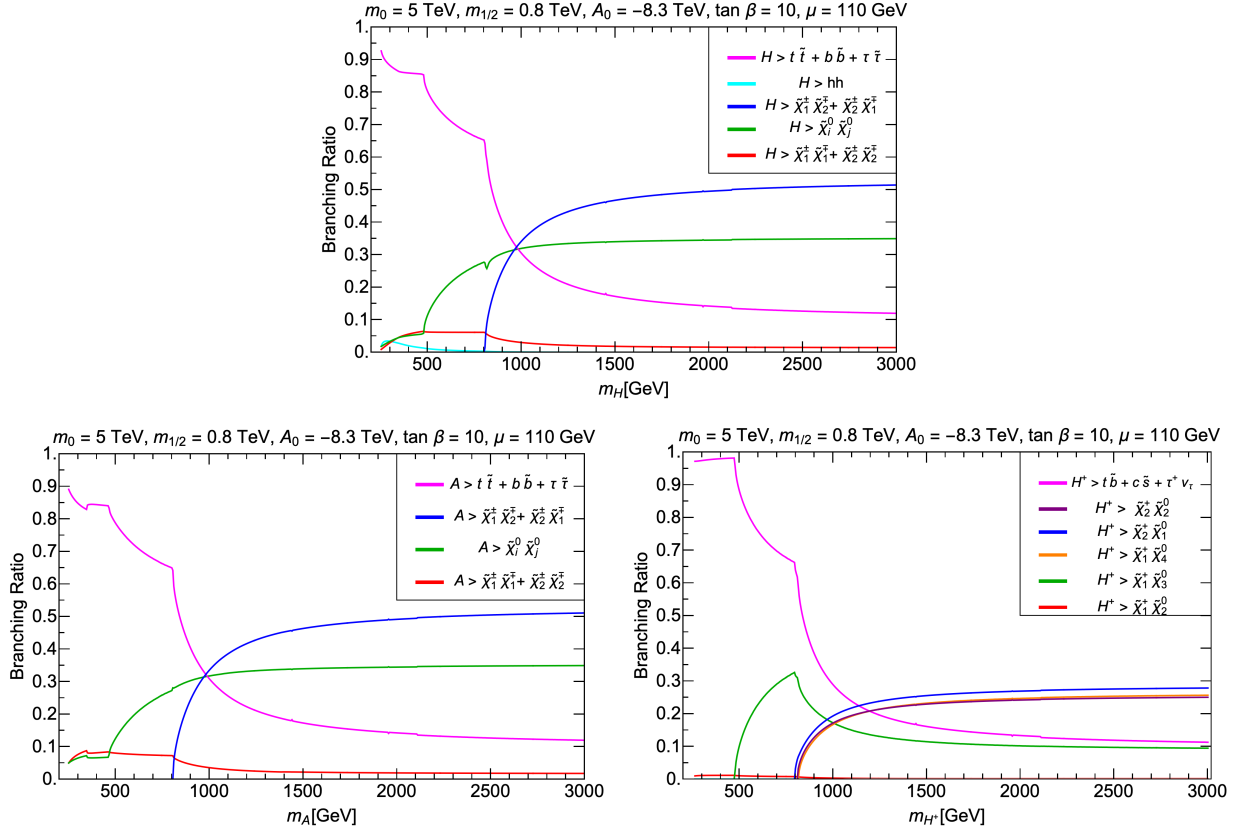


FIG. 3: Branching fractions versus heavy Higgs mass for a)  $H$ , b)  $A$  and c)  $H^+$  into SM and SUSY particles in the NUHM2 model with  $\mu = 200$  GeV and  $m_0 = 5$  TeV,  $m_{1/2} = 1$  TeV,  $A_0 = -8.3$  TeV and  $\tan \beta = 10$ .

In Fig. 3(b), we show the same branching fractions except now for the pseudoscalar  $A$ . The branching fractions look qualitatively similar to those in frame (a) since the same reasoning applies. Thus, the  $A$  will decay mainly to SM modes for smaller values of  $m_A$  even though decays to higgsino-like pairs are available. It is only when decays to gaugino plus higgsino opens up that the decay to SUSY modes begins to dominate.

For completeness, we also show in Fig. 3(c) the branching fractions for charged Higgs decays  $H^+$ . As in the previous cases,  $H^+$  decay to SM modes  $t\bar{b}$  and  $\tau^+\nu_\tau$  dominate at low values of  $m_{H^+}$  even though decay to  $\tilde{\chi}_1^+ \tilde{\chi}_{1,2}^0$  modes are kinematically allowed. As  $m_{H^+}$  increases, then decays to  $\tilde{\chi}_1^+ \tilde{\chi}_3^0$  (higgsino-bino) followed by  $\tilde{\chi}_2^+ \tilde{\chi}_{1,2}^0$  and  $\tilde{\chi}_4^0 \tilde{\chi}_1^+$  (higgsino-wino) turn on and rapidly dominate the decays.



Some dominant heavy neutral Higgs decay branching fractions are shown in Table II for the benchmark point shown in Table I. We see again that for the benchmark point the  $H$ ,  $A$  decays to SM modes are suppressed compared to decay rates into gaugino plus higgsino.

decay mode	BF
$H \rightarrow b\bar{b}$	22.5%
$H \rightarrow \tilde{\chi}_1^\pm \tilde{\chi}_2^\mp$	31.2%
$H \rightarrow \tilde{\chi}_2^0 \tilde{\chi}_4^0$	12.2%
$A \rightarrow b\bar{b}$	22.9%
$A \rightarrow \tilde{\chi}_1^\pm \tilde{\chi}_2^\mp$	30.0%
$A \rightarrow \tilde{\chi}_1^0 \tilde{\chi}_4^0$	12.2%

TABLE II: Dominant branching fractions for heavy Higgs  $H$ ,  $A$  for the benchmark point with  $m_A = 1200$  GeV.

In Fig. 4, we combine the  $H$ ,  $A$  production rates from Fig. 2 with the Higgs boson and sparticle branching fractions to the  $4\ell + \cancel{E}_T$  final state depicted in Fig. 1. We see from Fig. 4(a) that, for  $\tan\beta = 10$ , even without cuts we expect *at most*  $\sim 7$  signal events at HL-LHC, assuming an integrated luminosity of  $3000 \text{ fb}^{-1}$ . Moreover, we expect that this will be reduced considerably once detector efficiency and analysis cuts are folded in. However, as we can see from frame (b), the raw signal cross section is larger at the higher energy FCC-hh or SPPC by a factor 150-500 (compared to LHC14), so that with the projected  $15 \text{ ab}^{-1}$  of integrated luminosity, we may hope to be able to extract an observable signal even after cuts. We will, therefore, mostly focus our attention on a 100 TeV  $pp$  collider in the remainder of this paper.

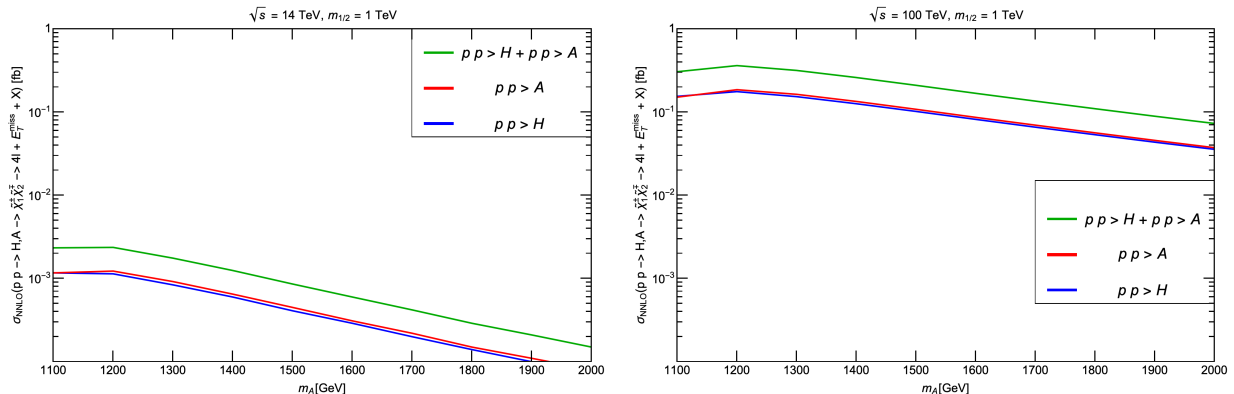


FIG. 4: NNLO Cross sections from SusHi  $\sigma(A)$ ,  $\sigma(H)$ , and  $\sigma(A) + \sigma(H)$  times the cascade decay branching fractions into the  $4\ell + \cancel{E}_T$  final state in fb vs.  $m_A$  for (a) 14 TeV and (b) 100 TeV without any cuts.

The reader may be concerned that our dismissal of the possibility of a signal in the  $4\ell + \cancel{E}_T$  channel at LHC14 was based on the event rate for  $\tan\beta = 10$  when it is well-known that the couplings of the  $A$  and  $H$  both increase with  $\tan\beta$ , resulting in an increased rate for  $H/A$  production from bottom quark fusion. It should, however, be remembered that the range of  $m_A$  excluded by the current upper limit on the cross section times branching ratio for the

decay  $\phi \rightarrow \tau\bar{\tau}$  ( $\phi = A, H$ ) also increases with  $\tan\beta$  for this same reason. This is illustrated in Fig. 5 where we show the expectations for the resonant production of tau pairs from the decay of  $H/A \rightarrow \tau\bar{\tau}$  versus  $m_A$  for several values of  $\tan\beta$ . Other parameters are taken to be the same as for the model-line introduced earlier. The horizontal black line is the current ATLAS upper bound on this rate [29]. We see that while  $m_A > 1.1$  TeV for  $\tan\beta = 10$ , for  $\tan\beta = 50$ ,  $m_A > 2$  TeV. Scaling the cross section in the left frame of Fig. 4 by the ratio of the corresponding values of  $\tan^2\beta$  still leaves us with just a handful of events *before cuts* at the HL-LHC for currently allowed values of  $m_A$ .

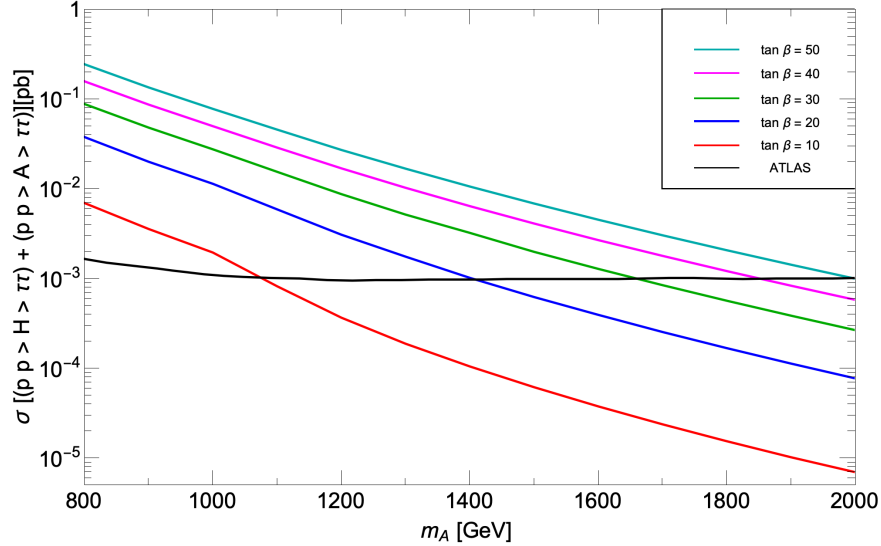


FIG. 5: The summed cross section times branching ratio for  $A/H \rightarrow \tau\bar{\tau}$  versus  $m_A$  at LHC14 for several values of  $\tan\beta$ . Other parameters are fixed at their values for the model line introduced in the text. The horizontal black line shows the current upper limit on the cross section obtained by ATLAS.

#### IV. SM BACKGROUNDS AND ANALYSIS CUTS

Our signal  $pp \rightarrow H, A \rightarrow \chi_1^\pm \chi_2^\mp \rightarrow 4\ell + \cancel{E}_T$  contains 4 leptons and missing energy in the final states, where one pair of leptons comes from the decay of a  $Z$ -boson. Since, as just mentioned, the signal rate is too small at the HL-LHC, we will from now on mostly focus our attention on a 100 TeV  $pp$  collider.

Our simplified study has been carried out at parton level. The dominant SM background to the  $4\ell + \cancel{E}_T$  events comes from  $W^\pm W^\mp V$ ,  $t\bar{t}V$ ,  $Zh$  and  $ZZV$  ( $V = W^\pm, Z, \gamma$ ). Notice that the partonic final states from the signal, as well as from all the backgrounds other than  $t\bar{t}V$  production, are free of any hadronic activity. We use tree-level matrix elements from the HELAS library in Madgraph to evaluate the backgrounds, and then scale our cross section to NLO with  $K$ -Factors calculated using MCFM [49].<sup>4</sup> For the  $t\bar{t}V$  background we veto

<sup>4</sup> The  $K$ -factors that we use are,  $K_{WWV} = 1.36$ ,  $K_{t\bar{t}V} = 1.30$ ,  $K_{Zh} = 1.40$  and  $K_{ZZV} = 1.40$ .

events which contain any  $b$ -jets (*i.e.*  $b$ -quarks) with  $p_T > 20$  GeV and  $|\eta(b)| < 2.5$ . This serves as a powerful cut in reducing this background. However, with PDF enhancements, we find that this background becomes the second most dominant background at  $\sqrt{s} = 100$  TeV.  $W^\pm W^\mp V$  proves to be the most dominant background at all energies.

To select events, we identify the isolated leptons if they satisfy

- $p_T(\ell_1, \ell_2, \ell_3, \ell_4) > 20$  GeV, 10 GeV, 10 GeV, 10 GeV;
- $|\eta|(\ell_1, \ell_2, \ell_3, \ell_4) < 2.5$ .

We model experimental errors in the measurement of lepton energies by Gaussian smearing electron and muon energies using [50],

$$\frac{\Delta E}{E} = \frac{0.25}{\sqrt{E(\text{GeV})}} \oplus 0.01, \quad (5)$$

where  $\oplus$  denotes addition in quadrature.

Since the signal of interest has a final state of  $4\ell + \cancel{E}_T$ , we started with a set of minimal cuts, labeled as **Cuts A**, which include :

- Veto events with  $b$ -jets  $p_T(\text{jet}) > 20$  GeV and  $|\eta|(\text{jet}) < 2.5$  as already mentioned;
- $\Delta_R(j, \ell) > 0.4$ , where  $j$  denotes a  $b$ -quark with  $p_T < 20$  GeV or with  $|\eta_b| > 0.4$ , to mimic lepton isolation;
- Invariant mass for two opposite sign same flavor leptons  $m_{\ell\ell} > 10$  GeV, to reduce the background from  $\gamma^* \rightarrow \ell\bar{\ell}$ ;
- $\cancel{E}_T > 125$  GeV.

After applying cut A, the mass distributions and  $\cancel{E}_T$  distribution obtained (upon summing  $b\bar{b}$  and  $gg$  initiated processes) are shown in Fig 6 and 7, respectively.

Since neutralinos and neutrinos escape detection (and so serve as sources of missing energy) it is not possible to reconstruct the invariant mass of  $H$  or  $A$  as a bump in the invariant mass of the final state. We can, however, sharpen the signal by additional cuts. Motivated by [51], we apply  $\cancel{E}_T \geq 275$  GeV cut, since we have two neutralinos of mass  $\sim 100$  GeV in the final state. As can be seen from Figs 6 and 7, the following mass cuts and  $\cancel{E}_T$  cuts can reduce the SM background very efficiently. Further cuts applied are :

- We define  $\ell_1$  and  $\ell_2$  as the two leptons whose invariant mass is closest to  $M_Z$  and require  $|M(\ell_1, \ell_2) - M_Z| < 10$  GeV since the signal includes one  $Z$  boson;<sup>5</sup>
- $10 < M(\ell_3, \ell_4) < 75$  GeV, where  $\ell_3$  and  $\ell_4$  denotes the remaining leptons.
- $0.14 m_A < M(4\ell) < 0.34 m_A$
- $\cancel{E}_T > 275$  GeV.

---

<sup>5</sup> Although we do not explicitly require it, for the most part,  $\ell_1$  and  $\ell_2$  have opposite sign and same flavour.

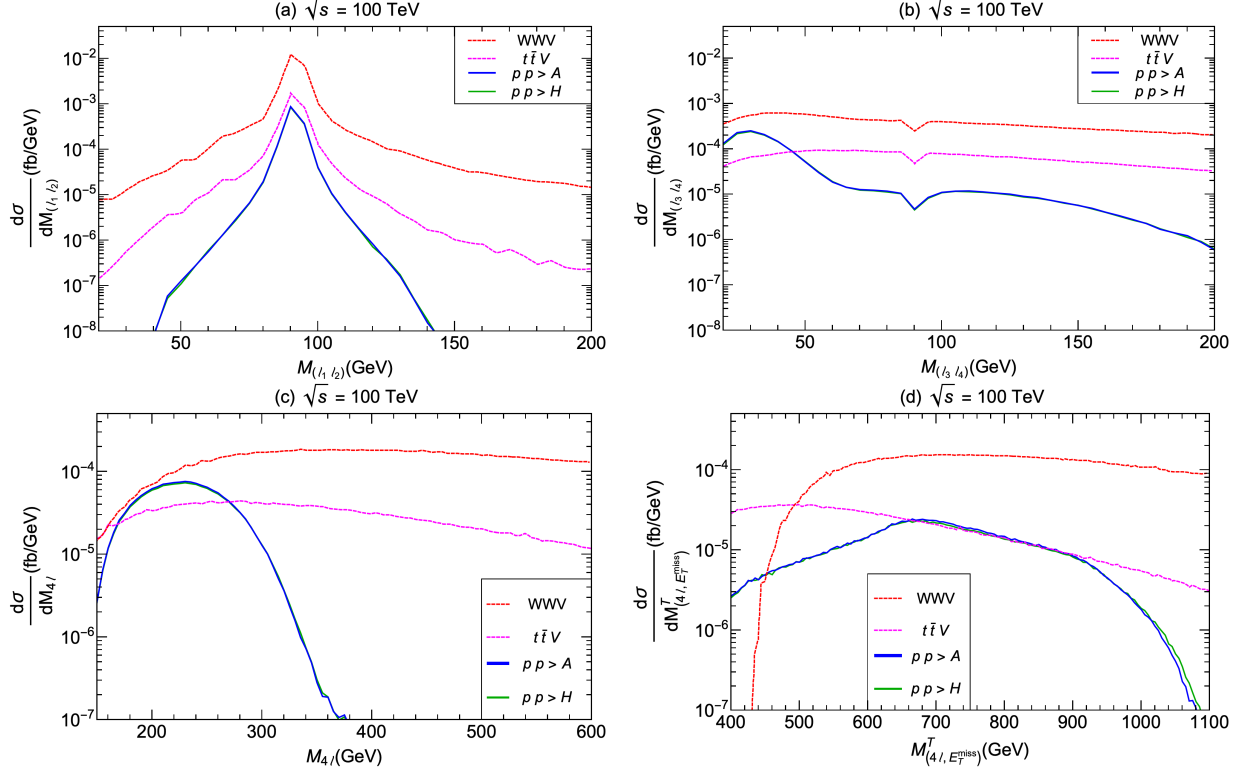


FIG. 6: Plots of the (a) invariant mass distribution  $M(\ell_1 \ell_2)$  of the two leptons that form an invariant mass closest to  $M_Z$ , (b) invariant mass distribution of the remaining two leptons,  $M(\ell_3, \ell_4)$ , (c) invariant mass of the  $4\ell$  system, and (d) cluster transverse mass distribution of the  $4\ell + \cancel{E}_T$  system, for the Higgs signal ( $pp \rightarrow H, A \rightarrow 4\ell + \cancel{E}_T + X$ ), after the cut set A defined in the text. The corresponding contributions from the dominant physics backgrounds are also shown.

Of course, since  $m_A$  is not *a priori* known, the cut on  $M(4\ell)$  needs further explanation. Unless  $m_A$  has already been measured from studies of  $A$  or  $H$  decays via SM channels, operationally,  $m_A$  here refers to the upper end point of the signal  $M_T(4\ell, \cancel{E}_T)$  distribution shown in frame (d) of Fig. 6, assuming that it can be experimentally extracted.<sup>6</sup> We note that the optimal choice of the  $M(4\ell)$  cut would only be weakly sensitive to the lightest neutralino mass for  $M_{A,H} \gg m_{\tilde{\chi}_1^0}$ . The cut set A, augmented by the cuts listed above, is labeled as cut **set B**.

In Fig. 8, we show the signal cross section versus  $m_A$  after cuts B at (a) the HL-LHC, and (b) a 100 TeV  $pp$  collider. We indeed see from frame (a) that for all values of  $m_A$  the signal lies well below the one event level. Although perhaps only of academic interest, it is worth noting that a comparison of this figure with Fig. 4(a) shows that the signal efficiency is  $\sim 5\text{-}10\%$  despite the requirement all four leptons are required to have a  $p_T$  of at least 10 GeV. This is a reflection of the boost the electroweakinos, and concomitantly the leptons,

<sup>6</sup> We appreciate that the extraction of this end point may be very difficult. Since this is a first exploration of the  $4\ell + \cancel{E}_T$  signal from the decay of heavy Higgs bosons in natural SUSY models, we do not attempt to explore the details of the end point determination, but simply assume that it can be extracted from the data.

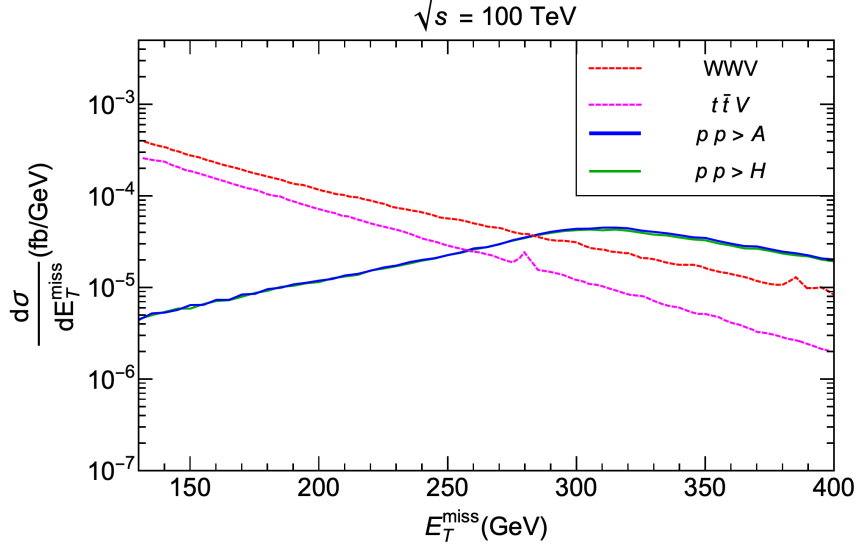


FIG. 7: The missing transverse energy  $\cancel{E}_T$  distribution for the Higgs signal ( $pp \rightarrow H, A \rightarrow 4\ell + \cancel{E}_T + X$ ) after the cuts set A. The corresponding contributions from the dominant physics backgrounds are also shown.

gain when they originate in the decays of the heavy Higgs bosons. From Fig. 8(b), we project that at the FCC or at the SPPC with an integrated luminosity of  $15 \text{ ab}^{-1}$ , several tens of signal events may be expected after cuts B over most of the range of  $m_A$  in the figure.

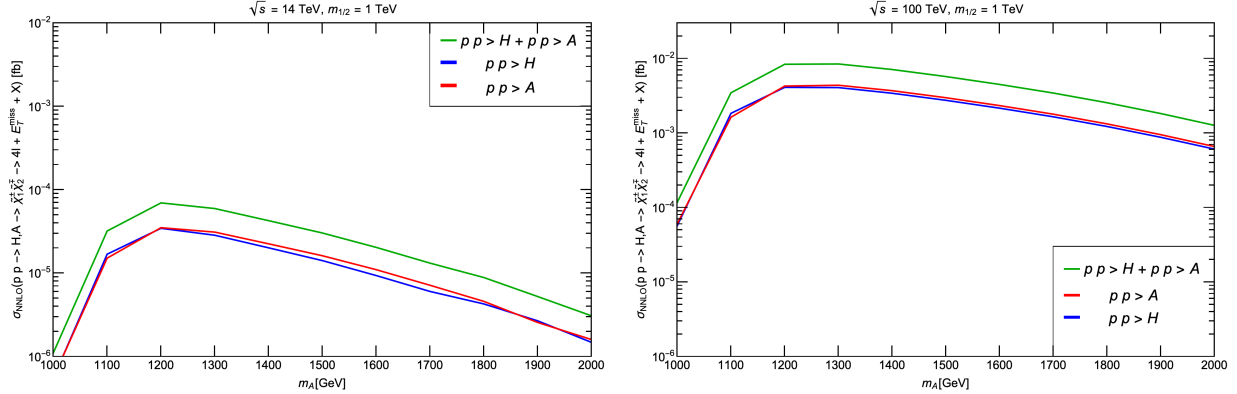


FIG. 8: NNLO Cross sections,  $\sigma(A)$ ,  $\sigma(H)$ , and  $\sigma(A) + \sigma(H)$  times the cascade decay branching fractions into the  $4\ell + \cancel{E}_T$  final state in fb vs.  $m_A$  for (a) 14 TeV and (b) 100 TeV, after the cut set B defined in the text.

## V. DISCOVERY POTENTIAL WITH CUT-AND-COUNT ANALYSIS

In this section, we study the discovery potential of the  $4\ell + \cancel{E}_T$  signal for heavy Higgs bosons at a 100 TeV  $pp$  collider using a traditional cut-and-count analysis. To this end, we show in Table III our results for the signal after the cut set B for three benchmark points

(BPs) with varying  $m_A$  (with other parameters fixed to their values in Table I), along with the main sources of SM backgrounds. The subdominant background listed in the fourth-last row is the combined background resulting from SM  $Zh$  and from  $ZZV$  production.

	BP1 $m_A = 1200$ GeV	BP2 $m_A = 1400$ GeV	BP3 $m_A = 1600$ GeV
$pp \rightarrow H$	$4.12 \times 10^{-3}$	$3.45 \times 10^{-3}$	$2.17 \times 10^{-3}$
$pp \rightarrow A$	$4.38 \times 10^{-3}$	$3.73 \times 10^{-3}$	$2.35 \times 10^{-3}$
$W^+W^-\ell^+\ell^-$	$7.13 \times 10^{-3}$	$7.23 \times 10^{-3}$	$6.18 \times 10^{-3}$
$t\bar{t}\ell^+\ell^-$	$1.83 \times 10^{-3}$	$1.58 \times 10^{-3}$	$1.17 \times 10^{-3}$
$Z\ell^+\ell^-\ell^+\ell^-$	$1.38 \times 10^{-3}$	$1.41 \times 10^{-3}$	$1.24 \times 10^{-3}$
$N_S$	127	108	68
$N_B$	155	153	129
$N_{ss}$	9.1	7.9	5.5

TABLE III: The signal and SM backgrounds at a 100 TeV  $pp$  collider for three benchmark points after the cut set B defined in the text. All the cross sections are in fb. Here,  $N_S$  is the total number signal events, combining both scalar and pseudo scalar and  $N_B$  is the total number of background events and  $N_{ss}$  is the statistical significance of the signal, all for an integrated luminosity of  $15 \text{ ab}^{-1}$ . We have all flavours of leptons ( $e$  and  $\mu$ ).

In Fig. 9, we present our estimates of statistical significance [52],

$$N_{ss} \equiv \sqrt{(2 \times (N_S + N_B) \ln(1 + N_S/N_B) - 2 \times N_S)},$$

for  $1100 \text{ GeV} \leq M_A \leq 2000 \text{ GeV}$ . Our selection cuts work well in removing a large part of the background. We see that with a center of mass energy of 100 TeV and integrated luminosity of  $\mathcal{L} = 15 \text{ ab}^{-1}$ , we have enough events to claim a  $5\sigma$  discovery for  $m_A \sim 1.1 - 1.65$  TeV. We also obtain a 95% CL exclusion limit for the  $H, A \rightarrow 4\ell + \cancel{E}_T$  signal for values of  $m_A$  extending out as far as 2 TeV.

We now turn to an examination of whether we can use machine learning techniques to suppress the background further and concomitantly increase the reach. In the next section, we study the use of boosted decision trees to further enhance the signal.

## VI. IMPROVEMENT WITH BOOSTED DECISION TREES

We have just seen that the cut-based signal from heavy Higgs boson decays via the  $4\ell + \cancel{E}_T$  channel yields a statistically significant discovery level over a limited range of  $m_A$  values even at a 100 TeV  $pp$  collider. Of course, it is possible that this signal may be combined with a signal from other channels to claim discovery over a wider range. The point of this study, however, is to examine how much improvement may be possible without combining other channels if we go beyond the traditional cut-based analysis which as we saw yields a discovery significance of  $N_{ss} > 5$  for  $m_A \sim 1.1 - 1.65$  TeV for  $\sqrt{s} = 100$  TeV and  $15 \text{ ab}^{-1}$  of integrated luminosity.

It has been found that ML techniques can greatly improve the signal-to-background discrimination and they are widely used by experimental analyses. In this section we use



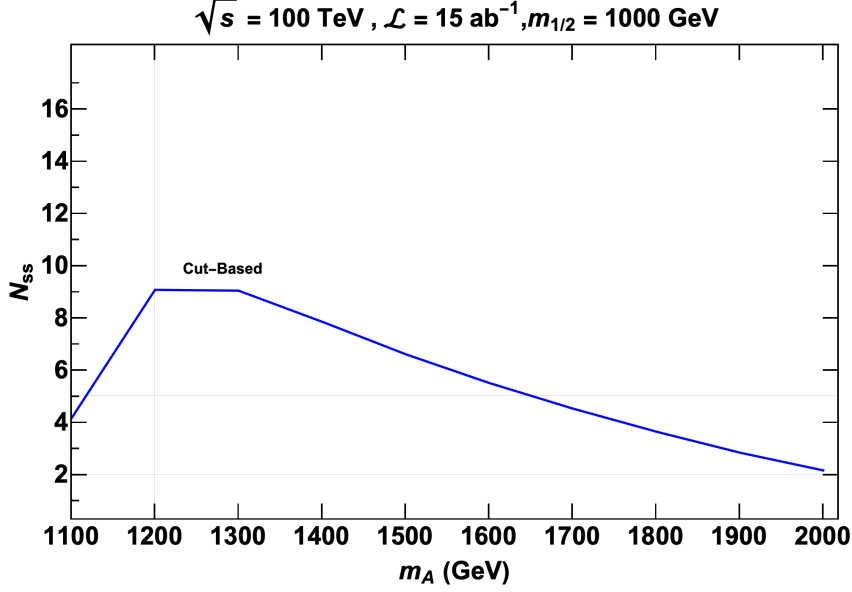


FIG. 9: The signal significance  $N_{ss}$  vs  $m_A$  using a traditional cut-based analysis for  $pp \rightarrow H + A \rightarrow 4\ell + \cancel{E}_T$  events at a 100 TeV  $pp$  collider.

boosted decision trees (BDT) for which algorithms are included in the ToolKit for Multi-Variate Analysis (TMVA) [53], a multivariate analysis package included with ROOT. For this study, we have used the following variables for training and testing,

- The invariant mass  $m(4\ell)$ .
- The invariant masses  $m(\ell_1, \ell_2)$  and  $m(\ell_3, \ell_4)$
- $\cancel{E}_T$ , missing transverse energy.

We have generated signal files for each value of  $m_A$  along with background at 100 TeV after applying the basic selection cuts and cuts on  $m(\ell_1, \ell_2)$ ,  $m(\ell_3, \ell_4)$  and  $\cancel{E}_T$  from the previous section. We combine all the backgrounds and train using signal files for different  $m_A$  values. In addition to cuts mentioned above, we require  $0.14 m_A \leq M(4\ell) \leq 0.34 m_A$  and  $\cancel{E}_T > 200$  GeV before passing the sample for training and testing. We train 400,000 signal events and 400,000 background events for each channel. We used the same number of events for testing. Figure 10 shows the BDT response for three BPs with different  $m_A$  values.

In Table IV, we present our estimate of  $N_{ss}$  from the BDT analysis for the same BP points as in Table III. We see that there is, indeed, a significant improvement over the previous cut-based analysis.

Fig. 11 shows the individual contributions from each of  $H$  and  $A$  for the BDT analysis along with the significance from the combined  $H$  and  $A$  signal. This may be compared to the significance shown in Fig. 9 for the traditional cut-and-count analysis. We see that by using the BDT analysis that we would be able to discover  $H$  and  $A$  at the  $5\sigma$  level via  $H, A \rightarrow 4\ell + \cancel{E}_T$  channel for  $m_A \sim 1 - 2$  TeV – a considerable improvement in range of  $m_A$  over the usual cut-based method!

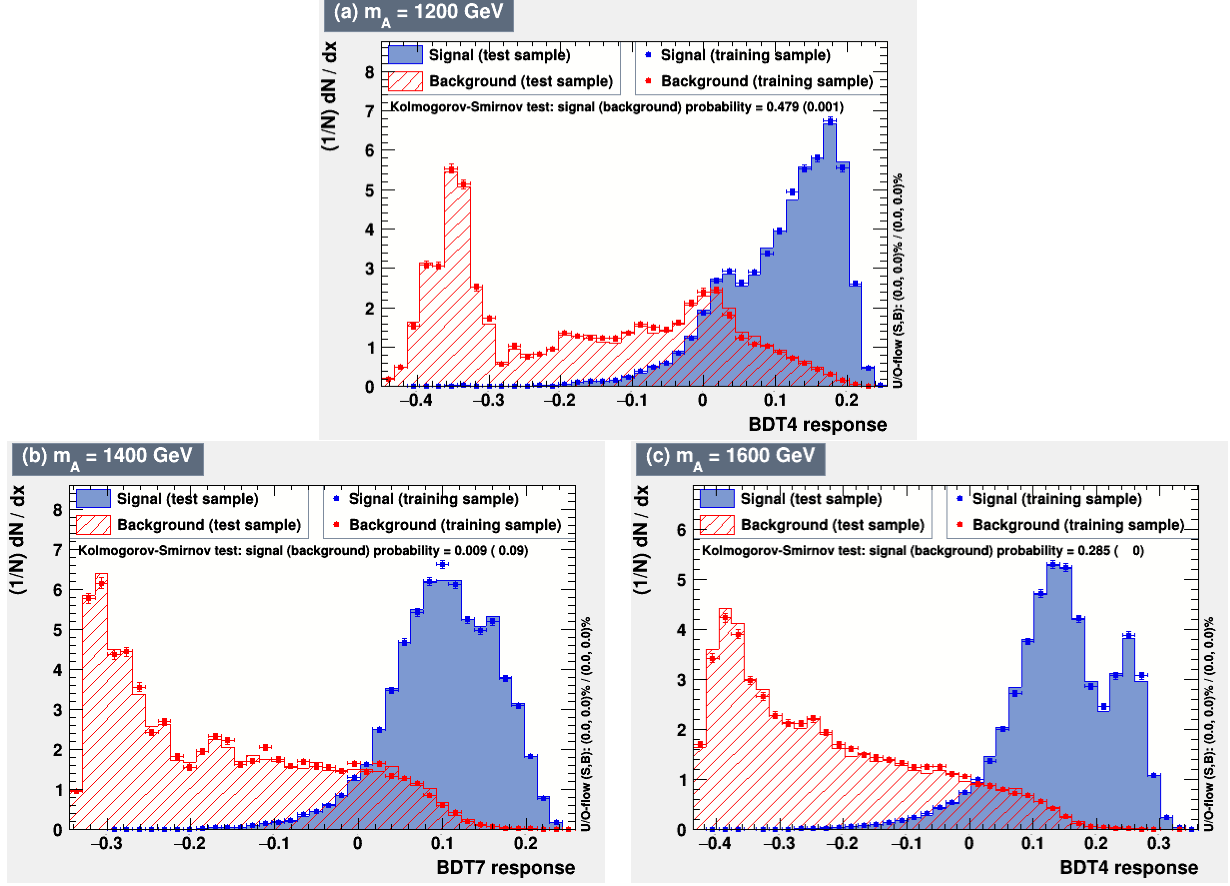


FIG. 10: The BDT response for  $m_A =$  (a) 1200, (b) 1400 and (c) 1600 GeV. The BDT response of test points (solid) and training points (with error bar) is superposed in the figure.

Number of Events	$pp \rightarrow \phi^0$	Total Background	$N_{ss}$
BP1, $m_A = 1200$ GeV			
All mass cuts	127	155	9.1
BDT cut	132	58	13.7
BP2, $m_A = 1400$ GeV			
All mass cuts	107	153	7.9
BDT cut	133	46	14.9
BP3, $m_A = 1600$ GeV			
All mass cuts	68	129	5.5
BDT cut	72	25	11.0

TABLE IV: A comparison between the cut based and BDT analyses for the three benchmark points introduced in the text.

## VII. CONCLUSIONS

In this paper, we have examined heavy neutral Higgs boson discovery as motivated by natural SUSY models with light higgsinos. In such models, the heavy Higgs  $H$ ,  $A$  decays to electroweakinos are almost always open since the lightest higgsinos are expected to have

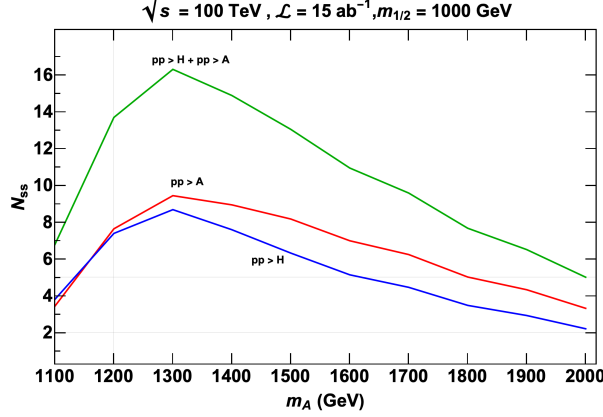


FIG. 11: Statistical significance plots for the  $H, A \rightarrow 4\ell + \cancel{E}_T$  signal at a 100 TeV hadron collider after the BDT analysis.

masses below  $\sim 350$  GeV range whilst the  $H$  and  $A$  bosons can have TeV-scale masses. Since decays to pairs of higgsino-like states are dynamically suppressed, our channel of primary interest is  $H, A \rightarrow \tilde{\chi}_1^\pm \tilde{\chi}_2^\mp$  decay, followed by  $\tilde{\chi}_2^\pm \rightarrow Z \tilde{\chi}_1^\pm$  followed by  $Z \rightarrow \ell^+ \ell^-$  and then each  $\tilde{\chi}_1^\pm \rightarrow \ell^\pm \nu_\ell \tilde{\chi}_1^0$ . Combining all flavours of decays to  $e$  and  $\mu$  leads to a distinctive  $H, A \rightarrow 4\ell + \cancel{E}_T$  signature for heavy Higgs boson decay to SUSY particles. The leptons from  $\tilde{\chi}_1^\pm$  decay are soft in the  $\tilde{\chi}_1^\pm$  rest frame but are boosted to higher energies due to the large  $m_{H,A}$  masses. Thus, we evaluated this signal channel against dominant SM backgrounds for both HL-LHC and for FCC-hh or SPPC with  $\sqrt{s} = 100$  TeV, applying judicious cuts on various combinations of invariant masses of the leptons, and also requiring  $\cancel{E}_T > 275$  GeV. Our selection requirements retain much of the signal while removing the physics background efficiently.

In our analysis we have focused on production of the heavy Higgs bosons with a mass ( $m_H \simeq m_A$ ) between 1 TeV and 2 TeV. While a signal (in the  $4\ell + \cancel{E}_T$  channel) is not likely to be observable at HL-LHC, prospects are much better at FCC-hh or SPPC. The best case for discovery is near  $m_A \simeq 1.2 - 1.3$  TeV that has a balance between kinematics of leptons in the final state and production cross sections. We note the following:

- A 100 TeV hadron collider offers promise to discover a heavy neutral Higgs boson via one of its dominant SUSY decay modes in natural SUSY models with a mass  $\sim 1 - 2$  TeV. With a conventional cut-based analysis, we are able to obtain a  $N_{ss} > 5$  statistical significance over a range  $m_A \sim 1.1 - 1.65$  TeV. We find though that a BDT analysis of the same signal can potentially improve the significance greatly giving  $N_{ss}$  as high as 16 for  $m_A \simeq 1.3$  TeV, and  $N_{ss} > 5$  over a range  $m_A \sim 1 - 2$  TeV even via our proposed very difficult discovery channel.
- For somewhat smaller values of heavy Higgs boson masses characterized by  $m_A \lesssim 1$  TeV, the signal cross section is suppressed both by smaller branching ratio into the SUSY mode, and also by a smaller boost of the daughter EWinos which, in turn, reduces the efficiency with which the softer leptons pass the cuts. Nonetheless, the heavy neutral SUSY Higgs bosons should be detectable in this range via SM decay modes such as  $H, A \rightarrow \tau \bar{\tau}$ .
- For increasing  $m_A$  values beyond  $\sim 1.3$  TeV, the Higgs production cross section be-

comes much smaller since the  $gg$  and  $b\bar{b}$  fusion production cross sections are increasingly suppressed.

- We stress that we have focused only on the signal from a difficult SUSY decay mode of the heavy Higgs boson with an eye to assessing how ML techniques could serve to enhance difficult-to-see signals. Hence we have not examined the possibility of combining SUSY modes or whether the discovery of a heavy Higgs boson might be possible from a study of its SM decays.

For  $m_A \simeq m_H$  significantly beyond 1 TeV and  $\tan \beta \sim 10-50$ , it may become increasingly challenging to search for heavy Higgs bosons via their decays into SM particles due to the diminished branching fractions to  $b\bar{b}$  and  $\tau\bar{\tau}$ , once the dominant SUSY decay channels become allowed. The chargino and neutralino discovery channel for heavy Higgs bosons at high energy hadron colliders offers an important opportunity to discover the heavy neutral Higgs bosons via their decay into EWinos. An upgrade to a 100 TeV hadron collider seems essential for heavy Higgs  $H$  and  $A$  discovery via the natural SUSY  $4\ell + \cancel{E}_T$  channel.

## Acknowledgement

We thank an anonymous referee for useful suggestions. This work was supported in part by the US Department of Energy, Office of High Energy Physics Grant No. DE-SC-0009956 and DE-SC-0017647. The work of DS was supported in part by the Ministry of Science and Technology (MOST) of Taiwan under Grant No. 110-2811-M-002-574, and work of RJ is supported by MOST 110-2639-M-002-002-ASP.

- 
- [1] G. Aad et al. [ATLAS Collaboration], Phys. Lett. B 716 (2012) 1; S. Chatrchyan et al. [CMS Collaboration], Phys. Lett. B 716 (2012) 30,
  - [2] E. Witten, Nucl. Phys. B 188, 513 (1981); R. K. Kaul, Phys. Lett. B 109, 19 (1982).
  - [3] S. Dimopoulos, S. Raby and F. Wilczek, Phys. Rev. D 24 (1981) 1681; U. Amaldi, W. de Boer and H. Furstenau, Phys. Lett. B 260, 447 (1991); J. R. Ellis, S. Kelley and D. V. Nanopoulos, Phys. Lett. B 260 (1991) 131; P. Langacker and M. x. Luo, Phys. Rev. D 44 (1991) 817
  - [4] L. E. Ibanez and G. G. Ross, Phys. Lett. B110, 215 (1982); K. Inoue et al. Prog. Theor. Phys. 68, 927 (1982) and 71, 413 (1984); L. Ibanez, Phys. Lett. B118, 73 (1982); H. P. Nilles, M. Srednicki and D. Wyler, Phys. Lett. B 120 (1983) 346; J. Ellis, J. Hagelin, D. Nanopoulos and M. Tamvakis, Phys. Lett. B125, 275 (1983); L. Alvarez-Gaume, J. Polchinski and M. B. Wise, Nucl. Phys. B **221**, 495 (1983). B. A. Ovrut and S. Raby, Phys. Lett. B 130 (1983) 277; for a review, see L. E. Ibanez and G. G. Ross, Comptes Rendus Physique 8 (2007) 1013.
  - [5] H. E. Haber and R. Hempfling, Phys. Rev. Lett. 66 (1991) 1815; J. R. Ellis, G. Ridolfi and F. Zwirner, Phys. Lett. B 257 (1991) 83; Y. Okada, M. Yamaguchi and T. Yanagida, Prog. Theor. Phys. 85 (1991) 1; For a review, see e.g. M. S. Carena and H. E. Haber, Prog. Part. Nucl. Phys. 50 (2003) 63.
  - [6] S. Heinemeyer, W. Hollik and G. Weiglein, Phys. Rept. **425** (2006), 265.
  - [7] The ATLAS collaboration [ATLAS Collaboration], ATLAS-CONF-2017-022.
  - [8] A. M. Sirunyan et al. [CMS Collaboration], Phys. Rev. D 97, no. 1, 012007 (2018); A. M. Sirunyan et al. [CMS Collaboration], Eur. Phys. J. C 77, no. 10, 710 (2017).

- [9] The ATLAS collaboration [ATLAS Collaboration], ATLAS-CONF-2017-037.
- [10] A. M. Sirunyan et al. [CMS Collaboration], arXiv:1706.04402 [hep-ex].
- [11] R. Barbieri and G. F. Giudice, Nucl. Phys. B **306**, 63 (1988).
- [12] S. Dimopoulos and G. F. Giudice, Phys. Lett. B **357** (1995), 573.
- [13] G. W. Anderson and D. J. Castano, Phys. Rev. D **52** (1995) 1693.
- [14] R. Kitano and Y. Nomura, Phys. Rev. D **73** (2006) 095004; M. Papucci, J. T. Ruderman and A. Weiler, JHEP **1209** (2012) 035.
- [15] N. Craig, arXiv:1309.0528 [hep-ph].
- [16] H. Baer, V. Barger and D. Mickelson, Phys. Rev. D **88**, 095013 (2013); A. Mustafayev and X. Tata, Indian J. Phys. **88** (2014) 991; H. Baer, V. Barger, D. Mickelson and M. Padeffke-Kirkland, Phys. Rev. D **89**, 115019 (2014).
- [17] H. Baer, V. Barger, P. Huang, A. Mustafayev and X. Tata, Phys. Rev. Lett. **109** (2012) 161802; H. Baer, V. Barger, P. Huang, D. Mickelson, A. Mustafayev and X. Tata, Phys. Rev. D **87** (2013) no.11, 115028.
- [18] H. Baer and X. Tata, *Weak Scale Supersymmetry: From Superfields to Scattering Events*, (Cambridge University Press, 2006).
- [19] H. Baer, V. Barger and M. Savoy, Phys. Rev. D **93** (2016) no.3, 035016.
- [20] H. Baer, V. Barger, J. S. Gainer, P. Huang, M. Savoy, H. Serce and X. Tata, Phys. Lett. B **774** (2017) 451.
- [21] K. J. Bae, H. Baer, V. Barger, D. Mickelson and M. Savoy, Phys. Rev. D **90** (2014) no.7, 075010.
- [22] H. Baer, M. Bisset, D. Dicus, C. Kao and X. Tata, Phys. Rev. D **47** (1993) 1062.
- [23] H. Baer, M. Bisset, C. Kao and X. Tata, Phys. Rev. D **50** (1994) 316.
- [24] F. Bordry, M. Benedikt, O. Brüning, J. Jowett, L. Rossi, D. Schulte, S. Stapnes and F. Zimmermann, [arXiv:1810.13022 [physics.acc-ph]].
- [25] M. Ahmad, D. Alves, H. An, Q. An, A. Arhrib, N. Arkani-Hamed, I. Ahmed, Y. Bai, R. B. Feroli and Y. Ban, *et al.* IHEP-CEPC-DR-2015-01.
- [26] [European Strategy Group], “2020 Update of the European Strategy for Particle Physics,” doi:10.17181/ESU2020
- [27] F. E. Paige, S. D. Protopopescu, H. Baer and X. Tata, hep-ph/0312045.
- [28] D. Matalliotakis and H. P. Nilles, Nucl. Phys. B **435** (1995) 115; M. Olechowski and S. Pokorski, Phys. Lett. B **344** (1995) 201; P. Nath and R. L. Arnowitt, Phys. Rev. D **56** (1997) 2820; J. Ellis, K. Olive and Y. Santoso, Phys. Lett. B **539** (2002) 107; J. Ellis, T. Falk, K. Olive and Y. Santoso, Nucl. Phys. B **652** (2003) 259; H. Baer, A. Mustafayev, S. Profumo, A. Belyaev and X. Tata, JHEP **0507** (2005) 065.
- [29] G. Aad *et al.* [ATLAS], Phys. Rev. Lett. **125** (2020) no.5, 051801.
- [30] G. Aad *et al.* (ATLAS Collaboration) Phys. Rev. D **101** (2020) 052005; A. Tumasyan *et al.* (CMS Collaboration) arXiv:2111.06296 (2021).
- [31] H. Baer, D. Dicus, M. Drees and X. Tata, Phys. Rev. D **36** (1987) 1363.
- [32] J. F. Gunion, H. E. Haber, M. Drees, D. Karatas, X. Tata, R. Godbole and N. Tracas, Int. J. Mod. Phys. A **2** (1987) 1035.
- [33] J. F. Gunion and H. E. Haber, Nucl. Phys. B **307** (1988) 445. [erratum: Nucl. Phys. B **402** (1993), 569].
- [34] K. Griest and H. E. Haber, Phys. Rev. D **37** (1988) 719.
- [35] Z. Kunszt and F. Zwirner, Nucl. Phys. B **385** (1992) 3.
- [36] A. Djouadi, P. Janot, J. Kalinowski and P. M. Zerwas, Phys. Lett. B **376** (1996) 220.

- [37] V. D. Barger, M. S. Berger, J. F. Gunion and T. Han, Phys. Rept. **286** (1997) 1.
- [38] G. Belanger, F. Boudjema, F. Donato, R. Godbole and S. Rosier-Lees, Nucl. Phys. B **581** (2000) 3.
- [39] S. Y. Choi, M. Drees, J. S. Lee and J. Song, Eur. Phys. J. C **25** (2002) 307.
- [40] C. Charlot, R. Salerno and Y. Sirois, J. Phys. G **34** (2007) N1.
- [41] M. Bisset, J. Li, N. Kersting, R. Lu, F. Moortgat and S. Moretti, JHEP **08** (2009) 037.
- [42] K. J. Bae, H. Baer, N. Nagata and H. Serce, Phys. Rev. D **92** (2015) no.3, 035006.
- [43] R. K. Barman, B. Bhattacharjee, A. Chakraborty and A. Choudhury, Phys. Rev. D **94** (2016) no.7, 075013.
- [44] E. Bagnaschi, H. Bahl, E. Fuchs, T. Hahn, S. Heinemeyer, S. Liebler, S. Patel, P. Slavich, T. Stefaniak and C. E. M. Wagner, *et al.* Eur. Phys. J. C **79** (2019) no.7, 617.
- [45] S. Gori, Z. Liu and B. Shakya, JHEP **04** (2019) 049.
- [46] A. Adhikary, B. Bhattacharjee, R. M. Godbole, N. Khan and S. Kulkarni, JHEP **04** (2021) 284.
- [47] R. V. Harlander, S. Liebler and H. Mantler, Comput. Phys. Commun. **184** (2013) 1605.
- [48] S. Dittmaier *et al.* [LHC Higgs Cross Section Working Group], doi:10.5170/CERN-2011-002 [arXiv:1101.0593 [hep-ph]].
- [49] R. Boughezal, J. M. Campbell, R. K. Ellis, C. Focke, W. Giele, X. Liu, F. Petriello and C. Williams, Eur. Phys. J. C **77**, no.1, 7 (2017).
- [50] The ATLAS collaboration[ATLAS Collaboration], ATLAS-PHYS-PUB-2013-004.
- [51] M. Aaboud *et al.* [ATLAS Collaboration], JHEP **1810** (2018) 180.
- [52] G. Cowan, K. Cranmer, E. Gross and O. Vitells, Eur. Phys. Jour. C **71** (2011) 1554.
- [53] A. Hocker, P. Speckmayer, J. Stelzer, J. Therhaag, E. von Toerne, H. Voss, M. Backes, T. Carli, O. Cohen and A. Christov, *et al.* [arXiv:physics/0703039 [physics.data-an]].